DOI: 10.15669/pnst.4.574

Progress in Nuclear Science and Technology
Volume 4 (2014) pp. 574-577

ARTICLE

Measurement of radioactive fragment production excitation functions of lead by 400 MeV/u carbon ions

Tatsuhiko Ogawa[a,b*], Mikhail N. Morev[c], Takeshi Iimoto[a] and Toshiso Kosako[a]

[a] *University of Tokyo, 2-11-16, Yayoi, Bunkyo-ku, Tokyo, 113-8656, Japan;* [b] *Japan Atomic Energy Agency, 2-4 Shirakata, Tokai-mura, Naka-gun, Ibaraki-ken, 319-1195, Japan;* [c] *Science and Engineering Center for Nuclear and Radiation Safety, d.2/8, korp. 5, ul. Malaya Krasnoselskaya, Moscow, 107140, Russia*

Depth distributions of radioactive fragments in a thick lead target exposed to 400 MeV/u carbon ions were measured to obtain isotopic production cross-sections of ^{Nat}Pb(^{12}C,x)X (X=^{46}Sc, ^{48}V, ^{54}Mn, ^{56}Co, ^{58}Co, ^{59}Fe, ^{75}Se, ^{83}Rb, ^{85}Sr, ^{113}Sn, ^{121}Te, ^{127}Xe, ^{133}Ba, ^{139}Ce, ^{143}Pm, ^{144}Pm, ^{146}Gd, ^{148}Eu, ^{149}Gd, ^{172}Hf and ^{175}Hf) reactions as excitation functions. The obtained fragment distributions were converted to excitation functions of fragmentation cross-sections by the modified stacked-foil method. This conversion procedure was validated by comparing the obtained data with the available thin target experimental data. The obtained cross-sections were in good agreement with the previously published results. Comparison of the obtained cross-sections and the simulation by PHITS showed that PHITS underestimates fragments lighter than 90 amu by factor of about 10 whereas the fragments heavier than 110 amu were predicted within a factor of 3. Energy and mass dependences of the obtained cross-sections give insight into the reaction mechanism and will be useful for radiation transport code benchmarking. Furthermore, this study clarified that excitation functions of fragmentation reactions induced by heavy ions can be obtained by applying the method adopted in this study.

Keywords: intermediate energy; fragmentation cross-section; excitation function; Monte-Carlo radiation transport simulation codes

1. Introduction

Heavy ion accelerators have been an indispensable tool for scientific research, industrial application and medicine for decades. Recently, the number of heavy ion accelerators is growing over the world for heavy ion cancer therapy [1]. Carbon ion beam of a few 100 MeV/u is most widely used among heavy ion beams.

For prediction of radiological impact in heavy ion accelerator facilities, radiation transport simulation codes play a fundamental role. The nuclear reactions are simulated by the combination of reaction models to describe physics in a wide energy range. However, the reaction models are sometimes inaccurate depending on energy. Therefore, it is necessary to verify the simulation codes in a wide energy range to apply them to various beam conditions.

A verification of the simulation codes has been performed for proton induced reactions and neutron induced reactions [2-4] based on abundant measured data whereas availability of data on heavy ion induced reactions is limited.

In this paper, we report on measurement of excitation functions of ^{Nat}Pb(^{12}C,x)X fragmentation reactions by the stacked-foil method. To validate the applicability of the method, a comparison of the measurement data with other available experimental data is discussed. The energy dependence of the measured excitation functions and comparison with cross-sections simulated with a radiation transport code are also discussed.

2. Methods

2.1. Principles of the method

The method adopted in this study to measure the excitation functions of fragmentation reactions is based on the stacked-foil method [5]. In this experiment, a stack of lead (99.99% purity) plates was irradiated by the focused 400 MeV/u carbon ion beam. The radioactive fragments in each lead plate were measured after the exposure by the gamma-spectrometry.

Contribution of secondary particles to formation of target fragments is usually an issue that hinders straight forward application of the stacked-foil method to measurement of excitation functions for heavy ions [6]. Nonetheless, target fragments other than fission fragments and target-like fragments were dominantly produced by incident heavy ions and secondary particle contribution is shown to be less than 20% and can be

*Corresponding author. Email: ogawa.tatsuhiko@jaea.go.jp

subtracted. Correction of measured cross-sections for secondary particle contribution is discussed in [7].

Assuming that contribution from secondary particles is negligible, the fragment production cross-sections are expressed by Eq. 1,

$$\sigma(E_n) = \frac{Y_n A}{N_A d \int_{t_{n1}}^{t_{n2}} \phi(t) dt} \quad (1)$$

where E_n is the average energy of primary ions in the middle of n-th target slice, Y_n (yield/sample) is the production of fragment nuclei, A is the atomic mass of the target material, N_A is the Avogadro constant, d is density of the target, t_{n1} is the coordinate of the upstream surface of n-th target slice, t_{n2} is the coordinate of the downstream surface of n-th target slice and $\phi(t)$ is the flux of primary ions at a depth of t inside target. Primary ion flux attenuation by depth was estimated based on the total reaction cross-section parameterization developed by Kox *et al* [8]. Energy of heavy ions in each target slice shown in **Figure 1** was calculated with ATIMA [9].

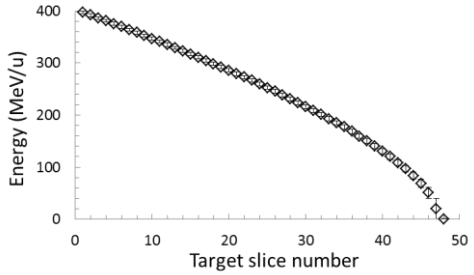

Figure 1. Primary ion energy in target slices

2.2. Experimental setup

The experiment was performed at the general-purpose irradiation room (PH1) of the Heavy Ion Medical Accelerator in Chiba (HIMAC) at the National Institute of Radiological Science (NIRS). The experimental geometry is illustrated in **Figure 2**.

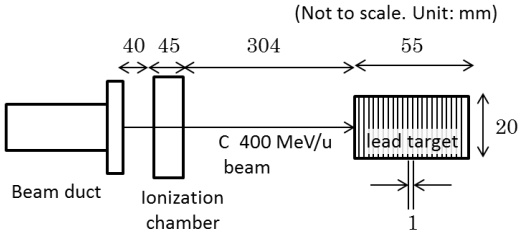

Figure 2. Schematic drawing of the experimental setup

The beam of 400 MeV/u ^{12}C ions was focused to less than 1 cm in diameter and directed normally to the geometrical center of the target surface. The target assembled as a stack of 55 circular lead plates of 0.1 cm thickness and of 2.0 cm diameter was placed 38.9 cm downstream the beam window. The absolute beam intensity integrated over the irradiation period was monitored by an air-filled plane-parallel ionization chamber placed immediately downstream the beam window. The fluctuation of beam intensity was monitored by a direct current to current transformer installed at the synchrotron ring. The measured yields Y' were normalized to the beam intensity by Eq. 2,

$$Y = Y' Exp(\lambda t_c) \frac{\int_0^{t_i} i(t) dt}{\int_0^{t_i} i(t) Exp(\lambda t_i - \lambda t) dt} \quad (2)$$

where Y is the yield corrected for decay and build-up, λ is the decay constant of the product, $i(t)$ is the beam intensity, t_i is the irradiation period (7.03 hours) and t_c (from 0.5 to 210 days) is the cooling period.

Gamma-ray spectra of the irradiated samples were measured with a high-purity germanium detector coupled to a spectroscopy-amplifier and a multichannel analyzer. The full-absorption peak efficiency for gamma-rays from 100 keV to 3000 keV was determined by a calibration procedure provided in [10].

Uncertainties of (1) gamma-ray count and sample thickness classified as random errors, (2) secondary particle contribution correction (7-24 %) and (3) primary ion beam intensity (0-5.5 %) were included to the plots as error bars. Uncertainties of (1) gamma-ray detection efficiency (3.1-12 %) and (2) absolute primary beam intensity monitored by the ionization chamber (3.6 %) classified as systematic errors are not shown in the plot. In addition to above uncertainties, gamma-ray full-absorption peak area involves an unaccounted uncertainty attributed to instability of peak shape.

3. Results and discussion

Some typical measured cross-sections are shown in **Figures 3-6**. The other data are provided elsewhere [7]. Horizontal error bars denote energy distribution (energy straggling and energy loss inside sample thickness) inside each sample. Yield type, independent (half-life of

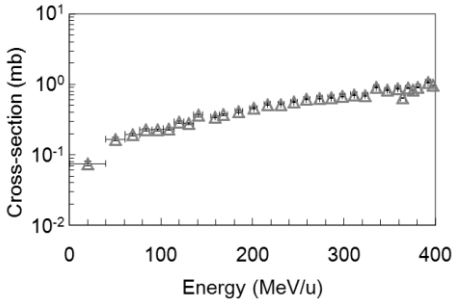

Figure 3. Excitation function of ^{Nat}Pb(^{12}C,x)^{46}Sc. Yield type is independent.

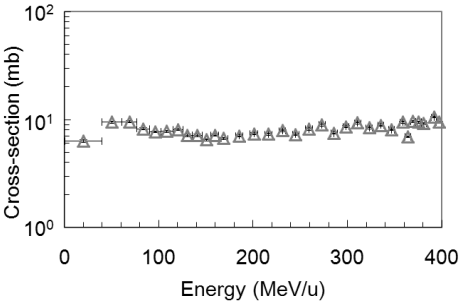

Figure 4. Excitation function of ^{Nat}Pb(^{12}C,x)^{75}Se. Yield type is cumulative.

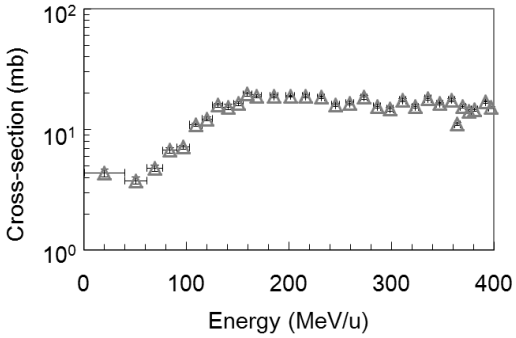

Figure 5. Excitation function of $^{Nat}Pb(^{12}C,x)^{143}Pm$. Yield type is cumulative.

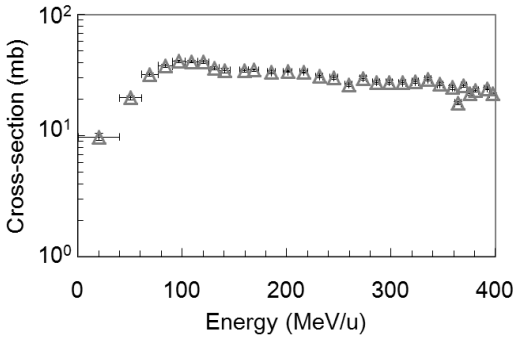

Figure 6. Excitation function of $^{Nat}Pb(^{12}C,x)^{172}Hf$. Yield type is cumulative.

progenitors are more than 10 times longer than the cooling period or no nuclear decay give contribution to the nuclide) or cumulative (half-life of progenitors are more than 10 times shorter than the cooling period), is given in the captions of each plot.

3.1. Comparison with literature data and simulated data

The cross-sections obtained in this study were compared with the measurement data available from literature to confirm the validity of this measurement.

Some isotopic production cross-sections of $^{Nat}Pb(^{12}C,x)$ reactions are provided by Yashima *et al.* [6] at a few energies and by Damdinsuren *et al.* [11] at 3.65 GeV/u. Available data are compared with our data and shown in **Figures 7, 8** and **9**. Cross-sections simulated by Monte-Carlo radiation transport code PHITS [12] are also shown.

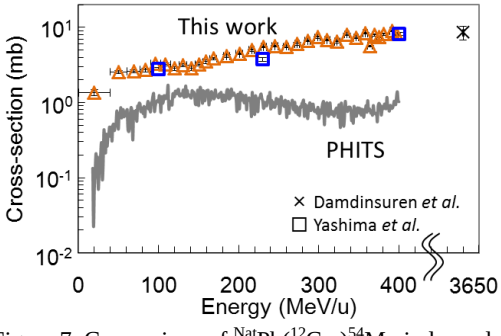

Figure 7. Comparison of $^{Nat}Pb(^{12}C,x)^{54}Mn$ independent cross-sections

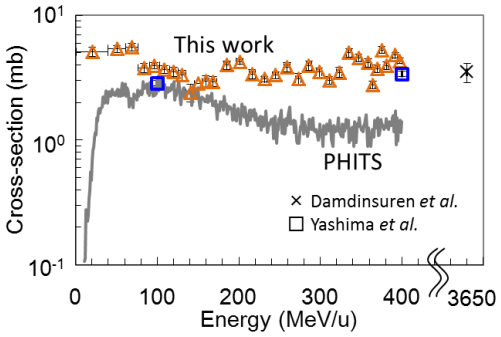

Figure 8. Comparison of $^{Nat}Pb(^{12}C,x)^{59}Fe$ cumulative cross-sections

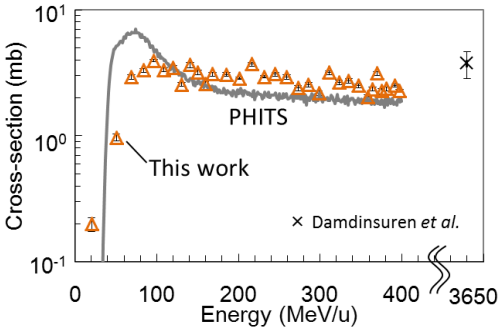

Figure 9. Comparison of $^{Nat}Pb(^{12}C,x)^{169}Yb$ cumulative cross-sections

The experimental data agree within the experimental uncertainty, which indicates the validity of this method. Importantly, the cross-sections at 100 MeV/u, affected by secondary particles in this study, is in good agreement with other experimental data.

PHITS underestimates products lighter than fission fragments such as ^{46}Sc and ^{59}Fe while products heavier than fission fragments are reproduced with better accuracy. With respect to energy, PHITS gives underestimation above 150 MeV/u or overestimation below 100 MeV/u therefore the shape of excitation functions agree no better than a factor of 2. More details on comparison between measured and simulated excitation functions are described elsewhere [7].

3.2. Shape of the excitation functions

The experimental data show cross-sections for light products (e.g. ^{46}Sc, ^{54}Mn) increase with increase of energy while the other cross-sections are energy-independent. It is also shown that the trend of fragmentation cross-sections changes near 150 MeV/u.

The comparison of experimental data with PHITS in Figures 7 and 8 indicates that there is a reaction mechanism not accounted in PHITS above 150 MeV/u which is responsible for production of light fragments. The increase of cross-sections with energy observed for production of ^{46}Sc and ^{54}Mn (but not in ^{59}Fe) may be explained by the unaccounted reaction mechanism.

4. Conclusion

We performed 400 MeV/u carbon ion irradiation to a thick lead target to measure excitation functions of $^{Nat}Pb(^{12}C,x)$ fragmentation reactions. The obtained data were compared with available literature data and simulation with a radiation transport code. Applicability of the stacked-foil method for measurement of excitation functions were confirmed by comparing the obtained cross-sections with the previous thin target measurements.

Excitation functions of $^{Nat}Pb(^{12}C,x)$ fragmentation reactions are obtained for various products except for fission fragments and target-like fragments. The shape of excitation functions depends on the product mass. PHITS agrees with the measurement data for nuclides heavier than fission fragments, however, irregular rise and dip in conflict with measurement data were observed.

Obtained cross-sections will be useful to benchmark energy dependence of nuclear reaction model performances and to obtain systematics of cross-sections for accurate prediction of radiological impact of high energy heavy ions.

Acknowledgements

We express gratitude to Dr. T. Murakami and the technical staff of NIRS-HIMAC for operating the HIMAC. This work was performed as a Research Project with heavy ions at NIRS-HIMAC.

This work was partly supported by a Grant-in-Aid for JSPS fellows.

References

[1] A. Kitagawa, T. Fujita, M. Muramatsu, S. Biri and A.G.Drentje, Review on heavy ion radiotherapy facilities and related ion sources, *Review of Scientific Instruments*, 81, (2010), 02B909.

[2] Yu. E. Titarenko, V. F. Batyaev, A. Yu. Titarenko, M. A. Butko, K. V. Pavlov, S. N. Florya, R. S. Tikhonov, S. G. Mashnik, A. V. Ignatyuk, N. N. Titarenko, W. Gudowski, M. Tesinsky, C.-M. L. Persson, H. Ait Abderrahim, H. Kumawat and H. Duarte, Cross sections for nuclide production in a ^{56}Fe target irradiated by 300, 500, 750, 1000, 1500, and 2600 MeV protons compared with data on a hydrogen target irradiated by 300, 500, 750, 1000, and 1500 MeV/nucleon ^{56}Fe ions, *Physical Review C*, 78, (2008), 034615.

[3] T. Sanami, M. Hagiwara, T. Oishi, M. Hosokawa, S. Kamada, Su. Tanaka, Y. Iwamoto, H. Nakashima and M. Baba, A Bragg curve counter with an internal production target for the measurement of the double-differential cross-section of fragment production induced by neutrons at energies of tens of MeV, *Nuclear Instruments and Methods in Physics Research Section A*, 610, (2009), pp. 660-668.

[4] Y. Iwamoto, S. Taniguchi, N. Nakao, T. Itoga, T. Nakamura, Y. Nakane, H. Nakashima, D. Satoh, H. Yashima, H. Yamakawa, K. Oishi, Y. Uwamino, A. Tamii, K. Hatanaka and M. Baba, Measurement of neutron spectra produced in the forward direction from thick graphite, Al, Fe and Pb targets bombarded by 350 MeV protons, *Nuclear Instruments and Methods in Physics Research Section A*, 562, (1997), pp. 789-792.

[5] R. Michel, R. Bodemann, H. Busemann, R. Daunke, M. Gloris, H. -J. Lange, B. Klug, A. Krins, I. Leya, M. Lüpke, S. Neumann, H. Reinhardt, M. Schnatz-Büttgen, U. Herpers, Th. Schiekel, F. Sudbrock, B. Holmqvist, H. Condé, P. Malmborg, M. Suter, B. Dittrich-Hannen, P. W. Kubik, H. A. Synal and D. Filges, Cross-sections for the production of residual nuclides by low- and medium-energy protons from the target elements C, N, O, Mg, Al, Si, Ca, Ti, V, Mn, Fe, Co, Ni, Cu, Sr, Y, Zr, Nb, Ba and Au, *Nuclear Instruments and Methods in Physics Research Section B*, 129, 2, (1997), pp.153-193.

[6] H. Yashima, Y. Uwamino, H. Iwase, H. Sugita, T. Nakamura, S. Ito and A. Fukumura, Cross sections for the production of residual nuclides by high-energy heavy ions, *Nuclear Instruments and Methods in Physics Research Section B*, 226, (2004), pp.243-263.

[7] T. Ogawa, M. N. Morev, T. Sato, M. Hashimoto and K.Niita, Analysis of fragmentation excitation functions of lead by carbon ions up to 400 MeV/u, *Nuclear Instruments and Methods in Physics Research Section B*, 300, (2013), pp.35-45.

[8] S. Kox, A. Gamp, C. Perrin, J. Arvieux, R. Bertholet, J. F. Bruandet, M. Buenerd, R. Cherkaoui, A. J. Cole, Y. El-Masri, N. Longequeue, J. Menet, F. Merchez and J. B. Viano, Trends of total reaction cross-sections for heavy ion collisions in the intermediate energy range, *Physical Review C*, 35, 5, (2004), pp.1678-1691.

[9] H. Geissel, Ch. Scheidenberger, P. Malzacher and J. Kunzendorf, <http://www-linux.gsi.de/~weick/atima/>.

[10] M. Morev, T. Ogawa and T. Kosako, An implementation of internal efficiency calibration method for γ-ray spectrometry analysis of activated samples, *Poster Session Proceedings of the Second Anniversary Symposium of GoNERI's Foundation*, Tokyo Japan, Oct. (2009), pp.157-162.

[11] C. Damdinsuren, V. I. Ilyushchenko, P. Kozma and D. Chultem, Yields of radionuclides formed in the interaction of 3.65 AGev 12C-ions and protons with ^{nat}Pb, *JINR Report*, (1989), pp. E1-89-481.

[12] K. Niita, N. Matsuda, Y. Iwamoto, H. Iwase, T. Sato, H. Nakashima, Y. Sakamoto and L. Sihver, *PHITS: Particle and Heavy Ion Transport Code System Version 2.23*, JAEA-Data/Code 2010-022, (2010).